

Visible Light Driven Photocatalytic Activity of Modified Glutamic acid-g-C₃N₄ and Polyaniline-g-C₃N₄ Composites

M. Jeba Jeeva Rani ^[1], G.Allen Gnana Raj ^[2]

Department of Chemistry and Research Centre
Scott Christian College (Autonomous), Nagercoil
Tamil Nadu - India.

ABSTRACT

Glutamic acid-g-C₃N₄ (CNA) and Polyaniline- g-C₃N₄ (CNPANI) composite samples have been synthesized by co-polymerization and oxidative polymerization method. The crystal structure, morphology and the elemental composition of the resulting composite samples were characterized by X-ray diffraction (XRD) spectroscopy, Fourier transform infrared spectroscopy (FT-IR), Scanning electron microscopy (SEM) and Energy dispersive X-ray analysis (EDAX). The optical properties of the composites have been explained by UV-Visible absorption spectroscopy. The photocatalytic activities of the prepared samples were evaluated using Rhodamine-B as the model pollutant. The results show that the CNA composite exhibit obviously enhanced photocatalytic performance under sunlight irradiation than CNPANI composite.

Keywords:- Carbon nitrate, Composite, Glutamic acid, Rhodamine B, Polyaniline.

I. INTRODUCTION

Globally, environmental pollution and energy problem causes serious mystery to the survival of life on the earth. Among all the pollution causing effects, waste water released from different textile industry is one of the most important causes [1]. And another important source of water contamination is the disposal of dye pollutants mainly from the pigment, leather, food and paper industries etc. Among them waste water generated by the entire synthetic dye to the ecosystem causes aesthetic pollution, eutrophication and perturbations in aquatic life [2]. These effluents contain a large amount of azoic, anthraquinonic, triphenylmethane and hetero poly aromatic dyes [3]. The discharge of highly pigmented hazardous dyes and other toxic organic compounds can be frequently removed by various methods [4] such as physical, chemical and biological treatment and also some techniques which are based on high energy UV light have been used [5]. However, these techniques are nondestructive and they convert an organic compound from one phase to another which requires further treatment to avoid secondary pollution. In order to overcome these drawbacks, the new oxidation technology known as Advanced oxidation processes (AOPs), especially heterogeneous photocatalysis with visible light is the most effective process for the degradation of various organic compounds and dyes. The efficient use of solar light based photocatalytic reaction is clean and strengthen to environment.

The new material discussed here consists exclusively of covalently linked, sp² hybridized carbon and

nitrogen atoms. It was suggested as graphitic carbon nitride (g-C₃N₄), by similar with structurally related graphite [6]. The metal-free organic photocatalysts can work in visible light and has high thermal and chemical stability as well as attractive electronic and optical properties. Nevertheless, the photocatalytic efficiency of bulk g-C₃N₄ is limited because of its low surface area and the fast recombination rate of photogenerated electron-hole pairs. To bring off these problems, numerous approaches have been involved to modify the bulk g-C₃N₄ such as band gap modification heteroatoms doping, post-functionalization and semiconductor coupling [7]. In recent years, the interest in the development of organic/polymer composite material has grown due to a wide range of applications, it exhibit absolutely different electronic and optical properties from those of bulk state.

In the present work has been planned an alternative energy devices such as glutamic acid-g-C₃N₄ and PANI-g-C₃N₄ metal-free composite photocatalysts that has complementary behavior between organic/polymer- g-C₃N₄ composites, it has been used for the removal of Rh-B dye in aqueous solution.

II. MATERIALS AND METHOD

Melamine, glutamic acid, aniline monomer, ammonium persulphate (APS) were purchased from Sigma-Aldrich. All other reagents were of analytical grade and were used as without further purification.

2.1 Synthesis of Photocatalysts

The metal free graphitic carbon nitride ($g\text{-C}_3\text{N}_4$) powder was synthesized by thermal treatment of precursor melamine it was placed in a crucible with a cover under ambient pressure in air. After dried at 80 °C for 24 h, the precursor was put in a Muffle furnace and heated to 550 °C for 3 h with a heating rate of 10 °C min^{-1} . The resultant pale yellow product was collected and ground into a powder for further use.

2.1.1 Synthesis of Glutamic acid- $g\text{-C}_3\text{N}_4$ (CNA) Composite

Amino acid doped $g\text{-C}_3\text{N}_4$ was obtained by co-polymerization method. 5 g $g\text{-C}_3\text{N}_4$, 0.5 g glutamic acid was taken in a beaker contain 150 ml deionized water, 7 ml 1 M HCl and ammonium persulphate (0.170 g) was added. After dispersing $g\text{-C}_3\text{N}_4$ and glutamic acid the resultant mixture was magnetically stirred for 3 h and allowed to polymerize for 3 h. The resultant yellow CNA composite sample was filtered and washed with ethanol and deionized water. The mixture was dried at 80 °C for 1 h in vacuum environment.

2.1.2 Synthesis of PANI- $g\text{-C}_3\text{N}_4$ (CNPANI) Composite

The pure $g\text{-C}_3\text{N}_4$ composite was prepared according to the procedure mentioned above. PANI- $g\text{-C}_3\text{N}_4$ composite photocatalyst was synthesized by oxidative polymerization of aniline monomer. A fixed amount of $g\text{-C}_3\text{N}_4$ (2 g), ammonium persulphate (0.068 g) (APS) and 1 M HCl (3ml) solution were added into 60 ml of deionized water in a beaker. The mixed solution was magnetically stirred for 1 h in an ice water bath. After that, aniline monomer (0.2 ml) was injected drop wise to the above cooled mixture. The resultant mixture was allowed to react in the ice bath for 8 h. The precipitated emerald green CNPANI composite powder was filtered and washed with ethanol and deionized water until the filtering solution becomes colourless. Finally, the product was dried in a vacuum environment.

2.2 Characterization of Photocatalyst

X-ray diffraction (XRD) analysis was carried out at room temperature with a Bruker D8 advance diffractometer. The patterns were run with Cu $K\alpha$ radiation at a scan rate of 20-80 °C. UV-Visible spectral data were collected over a spectral range 200-800 nm with Shimadzu UV-3101 PC spectrophotometer. Fourier transform-Infra red spectra (FT-IR) in transmittance mode were recorded for a solid mixture of sample and KBr in the form of pellets on a SHIMADZU FTIR spectrometer in the frequency range 4000 to 400 cm^{-1} with a spectral resolution of 16 (1 cm^{-1}) and an accumulation of 70 scans at room temperature. Scanning electron microscope (SEM) analysis was performed on platinum coated samples using a JOEL apparatus model

JSM-5610 LV. Elemental analysis was performed by energy dispersive X-ray micro analysis (EDAX) using BRUKER-10498 model instrument.

2.3 Measurement of photocatalytic activities

The photocatalytic degradation of Rh-B was performed under the natural sunlight in the presence of various types of composite photocatalysts. In the photocatalytic treatment of dye, a known concentration of Rh-B dye solution $1 \times 10^{-5}\text{M}$ (5 mg/l) was prepared in deionized water resulting in a solution with pH 7.6 was taken in a borosil glass beaker of 250 ml capacity. 0.1 g photocatalyst was added to the 50 ml (2 g/l) of dye solution. Before irradiation of the dye solution, the suspension was stirred for 30 min in the dark to realize adsorption-desorption equilibrium in the presence of catalyst. The concentration of substrate in bulk solution at this point was used as the initial value of the further kinetic treatment of photo degradation process. The dye solution was agitated with an electromagnetic stirrer at a constant speed of 790 rpm. The dye solution was directly exposed to sunlight radiation in an open atmosphere. At given intervals of irradiation a known volume of sample along with the catalyst particles were collected, centrifuged and then filtered through Millipore filter paper. The filtrates were analyzed by UV-Visible spectrophotometer. The determination wavelength is 553 nm for Rh-B dye, which is the maximum absorption wavelength.

The degradation efficiency of dye is calculated by the following equation

$$\text{Degradation efficiency (\%)} = \frac{C_0 - C}{C_0} \times 100$$

Where, C_0 is the initial concentration of dye before irradiation and C is the concentration of dye after a certain irradiation time.

III. RESULTS AND DISCUSSION

3.1 Characterization of metal free composite samples

Fig.1 and Fig. 2 shows the XRD patterns of CN and CNA composite samples. The intense peak at 27.7° is allocated to the crystallographic plane (002), an interlayer stacking of the conjugated aromatic segments in CN [8]. A weak peak which appears at around 13.2° becomes gradually reduced because non-metal atoms are only placed on the surface of the crystals. The average particle size of CNA is found to be in the nanometer range from the Scherrer's formula. The average crystalline size of CNA composites is found to be 7.8 nm respectively. Fig. 3 illustrates the XRD patterns of CNPANI composite sample. The pure $g\text{-C}_3\text{N}_4$ has two diffraction peaks at 27.5° and 13.1° , which can be

indexed as graphitic materials at the peaks (002) and (100). These two peaks are in good compatibility with the g-C₃N₄ reported in the literature [9]. In particular, no apparent diffraction peaks of PANI polymer is observed in CNPANI composite sample. This is due to the weak crystallinity and small doping content of PANI. However, in the presence of PANI in the composite can be confirmed by FT-IR and EDAX analysis.

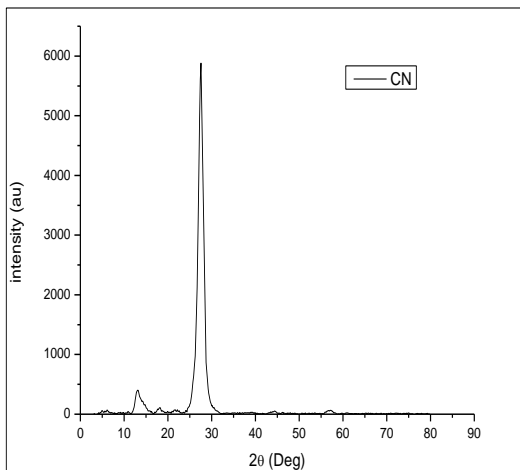


Fig. 1 XRD pattern of CN composite sample.

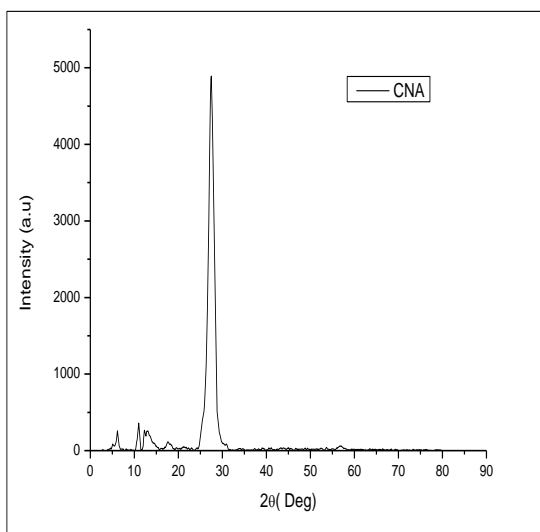


Fig. 1 XRD Pattern of CNA composite sample.

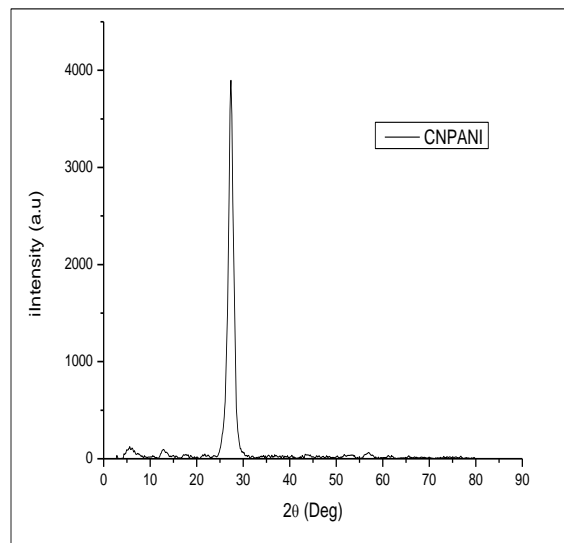


Fig. 3 XRD pattern of CNPANI composite sample.

Fig. 4 shows the FT-IR spectrum of CNA composite photocatalyst. The spectrum shows significant bands at 1242, 1327, 1411 and 1473 cm⁻¹, which can be represented as the stretching modes of C-N heterocyclic [10]. Moreover, the main characteristic bands of tri-azine units are at 802 and 887 cm⁻¹. The bands at 3271 and 3109 cm⁻¹ is due to the hydrogen bonded N-H between amine and imine sites. The above mentioned bands are the main characteristic peaks of g-C₃N₄ but an additional band at 1581 cm⁻¹ is due to C-O stretching vibration of acid group, the weak band at 1725 and 493 cm⁻¹ is due to C = O stretching and O-H in plane bending mode of acid [11]. This is the strong evidence that the interaction has been formed between glutamic acid and g-C₃N₄ composite sample.

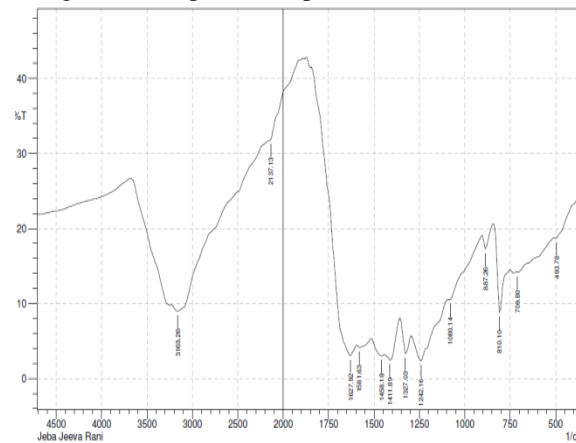


Fig. 4 FT-IR spectrum of CAN composite sample

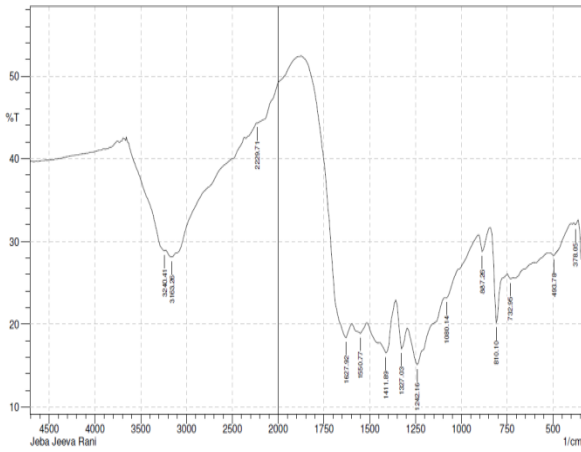


Fig. 5 FT-IR spectrum of CNA composite sample.

As shown in Fig. 5, all the characteristic features of the pure $g-C_3N_4$ are retained as already reported but an additional bands at 1550 and 1480 cm^{-1} is due to the $C = N$ and $C = C$ stretching vibrations of quinoid and benzenoid units of PANI [12]. In the presence of benzenoid and quinoid units are the evidences of the emaraldine form of PANI.

The CNA and CNPANI composite samples display micrometer size aggregated morphology as shown in Fig.6 and Fig.7 respectively. SEM images look like irregular agglomerates because of gases discharged from melamine deposition and also exhibits well dispersed crystals and the particle is homogeneous with the formation of fine dissipated particles.

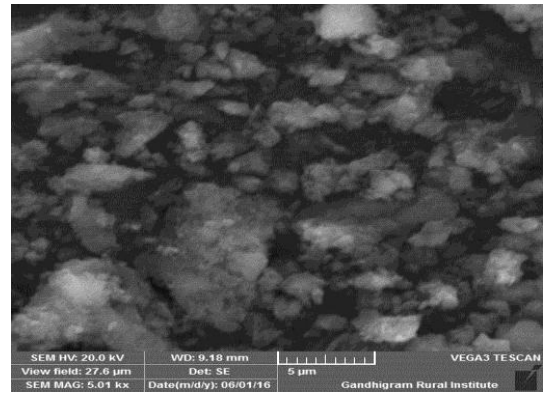
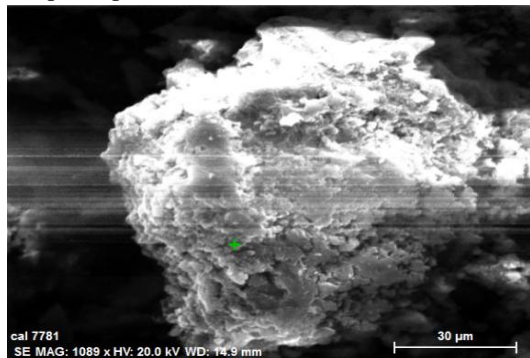


Fig. 6 SEM micrographs of CNA composite sample.

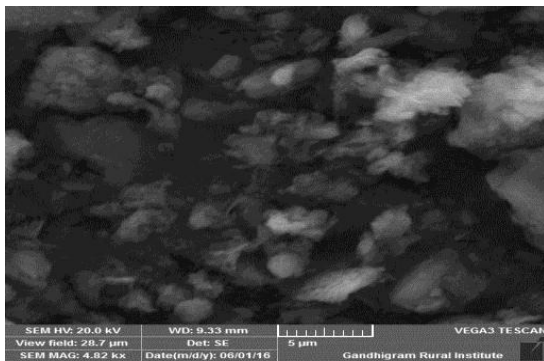
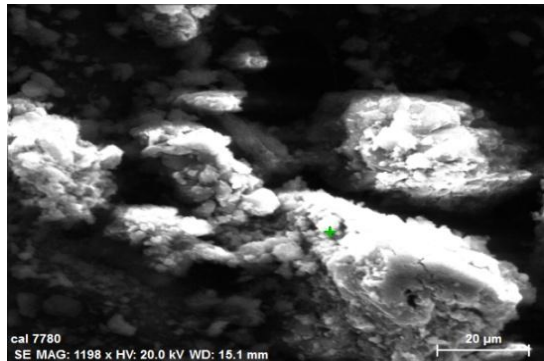


Fig.7 SEM micrographs of CNPANI composite sample.

Fig.8 and Fig.9 illustrates the EDAX analysis of the samples CND and CNA. The enhancement of weight % of C, N and O confirmed that the particles are deposited on the surface of CND and CNA composite samples and the composition of the samples in both atomic and weight percentage are tabulated in Table 1 and Table 2.

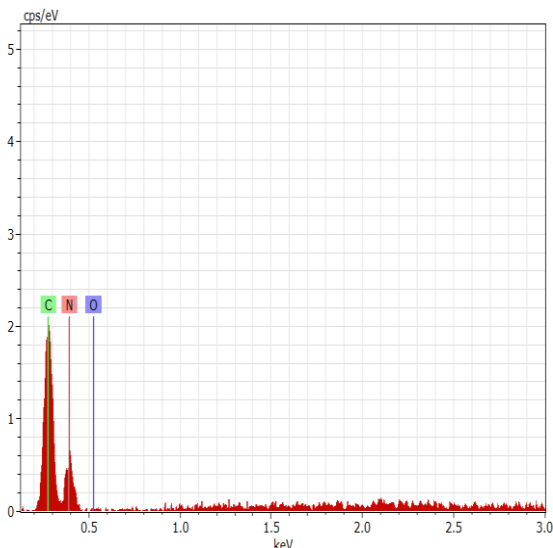


Fig.8 EDAX spectrum of CNA composite.

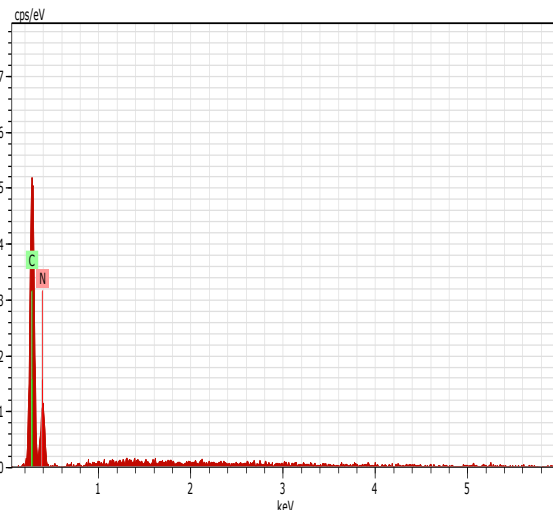


Fig.

9 EDAX spectrum of CNPANI composite.

Table 1 Atomic and weight percentage of CNA composite sample.

El AN	Series	unn. C [wt.%]	norm. C [wt.%]	Atom. C [at.%]	Error(1 Sigma) [wt.%]
N 7	K-series	58.15	58.15	54.53	17.98
C 6	K-series	40.73	40.73	44.55	8.69
O 8	K-series	1.12	1.12	0.92	1.79
	Total:	100.00	100.00	100.00	

Table 2 Atomic and weight percentage of CNPANI composite sample.

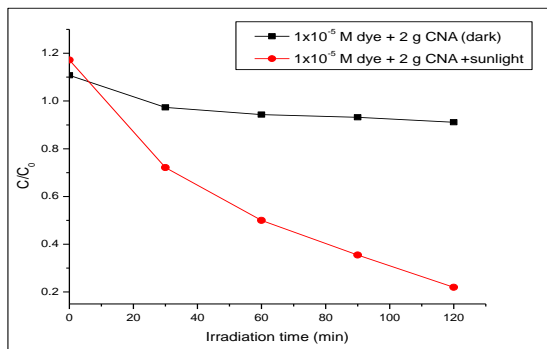
El AN	Series	unn. C [wt.%]	norm. C [wt.%]	Atom. C [at.%]	Error(1 Sigma) [wt.%]
N 7	K-series	54.95	54.95	51.13	13.79
C 6	K-series	45.05	45.05	48.87	7.71
	Total:	100.00	100.00	100.00	

3.2 Photocatalytic Activity

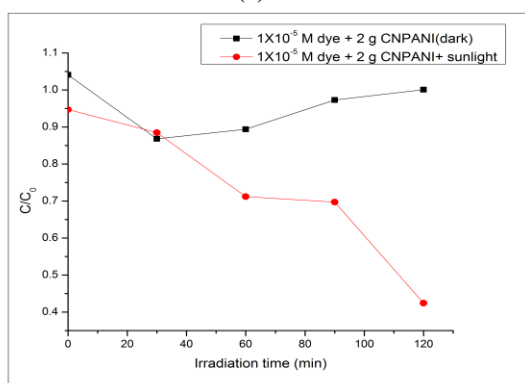
Photocatalytic degradation of Rh-B (1×10^{-5} M) in the presence of CNA and CNPANI composite photocatalysts under natural sunlight irradiation has been investigated. The characteristic absorption of Rh-B at 553 nm is used to monitor the photodegradation process. As can be seen in Fig. 10 (a) and (b) shows the photocatalytic activities of CNA and CNPANI composites under visible light

irradiation. The graph results evince that the degradation of dye in the presence of photocatalyst CNA but in the absence of sunlight is very low (9 %). When experiments are carried out in the presence of catalysts and sunlight, the rate of degradation is increased from 9 to 82 % respectively. In CNPANI, the absence of sunlight the percentage degradation of Rh-B is only about 3 % but in the presence of

sunlight and CNPANI, the rate of degradation increases from 3 to 55 % at 120 minutes irradiation.



(a)



(b)

Fig. 10 Effect of visible light on photodegradation of Rh-B over (a) CNA and (b) CNPANI composite photocatalysts.

The photocatalytic activities of CAN and CNPANI photocatalysts are evaluated by the degradation of the characteristic absorption peak of Rh-B at 553 nm. As shown in Fig. 11, there is a gradual decrease in intensity and the absorption peaks of Rh-B shifts from 553 nm to ~ 498 nm within 120 minutes irradiation. The result indicates that the degradation of Rh-B molecule especially the cleavage of the conjugated structure of the molecules. Fig.12 shows the degradation spectrum of Rh-B using CNPANI composite photocatalyst. Even when the irradiation time is prolonged to 120 minutes, the absorption peaks shifts from 553 nm to 480 nm. It indicates that only partial N-de-ethylation of Rh-B is obtained, it has been assumed that the Friedel-Crafts acylation of benzene like PANI dramatically affect the efficiency of the photocatalyst.

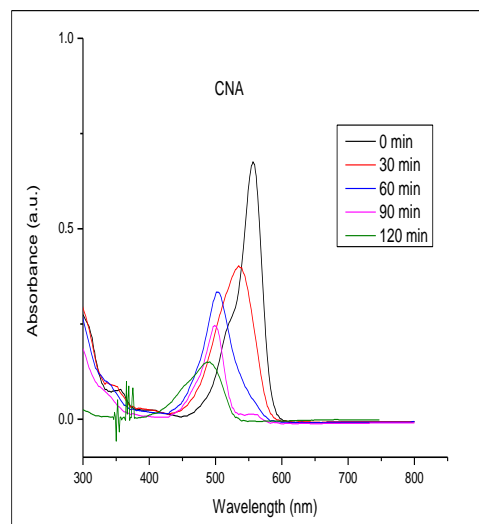


Fig. 11 Absorption peaks of Rh-B in CNA composite sample.

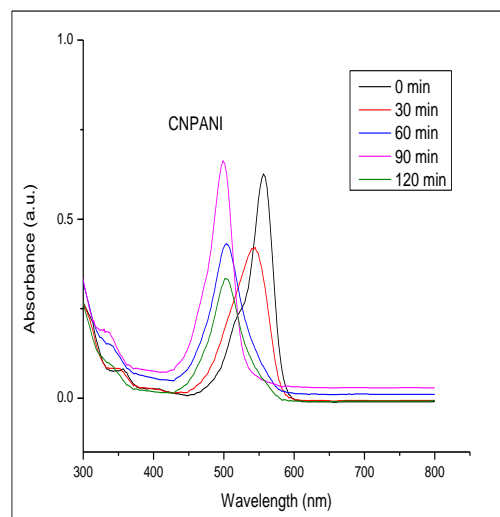
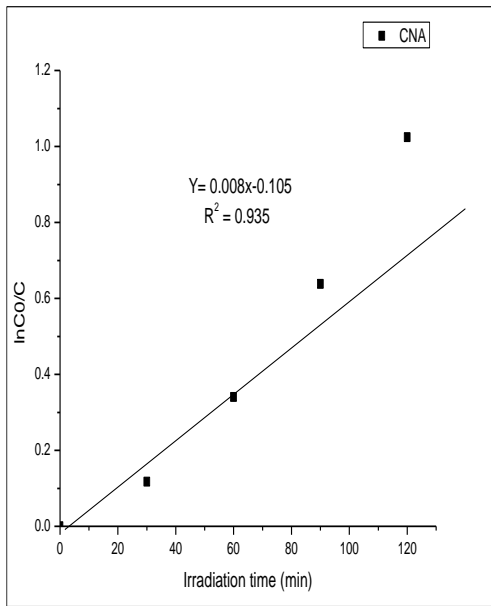


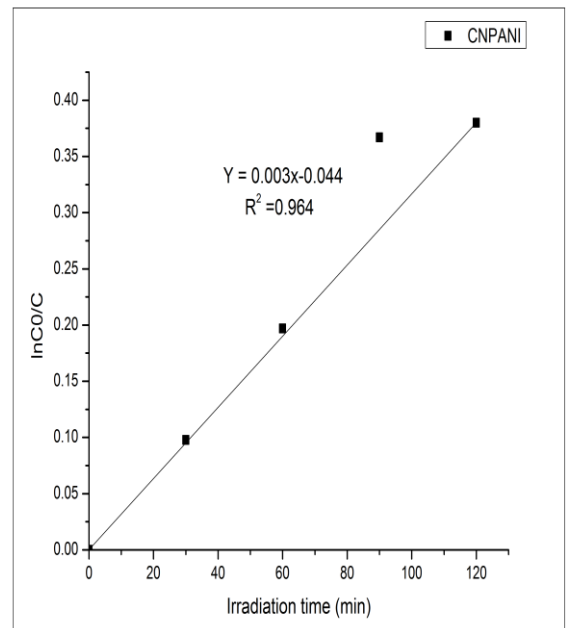
Fig. 12 Absorption peaks of Rh-B in CNPANI composite sample.

The kinetics of Rh-B dye on to CNA and CNPANI has been studied using first order kinetic model. Fig. 13 (a) and (b) displays the result of degradation rate of Rh-B using CNA and CNPANI photocatalysts. The photocatalytic degradation curves in both the cases fit well with pseudo-first order kinetics. The fitted lines are calculated to be $R^2 = 0.935$ for CNA and $R^2 = 0.964$ for CNPANI composite photocatalysts. The rate constants are calculated to be $0.014277 \text{ min}^{-1}$ for CNA and $0.006698 \text{ min}^{-1}$ for CNPANI composites. When compared to CNPANI the degradation rate constant of CNA composite can be estimated to be 2.13 times higher under the same reaction conditions. Therefore,

the CNA catalyst shows excellent photocatalytic activity than that of CNPANI.



(a)

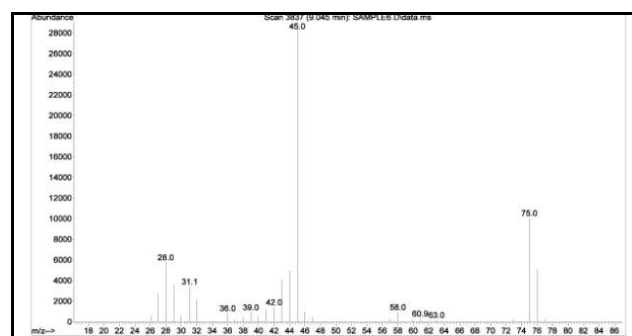
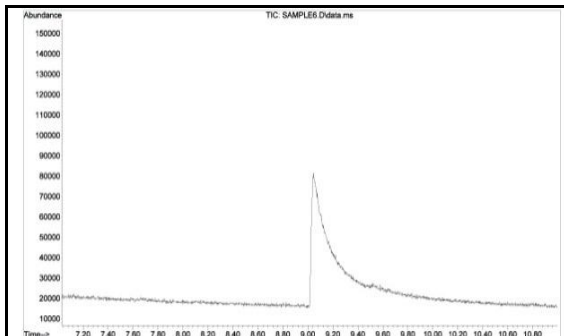


(b)

Fig.13 First-order plots for the photodegradation of Rh-B using (a) CNA and (b) CNPANI composite photocatalyst.

3.3 GC-MS Analysis

The investigation of the photodegradation products of Rh-B is achieved with the use of GC-MS chromatography. The GC-MS results of the final photodegradation products of Rh-B using sunlight and O₂ over CNA photocatalyst as shown in Fig.14



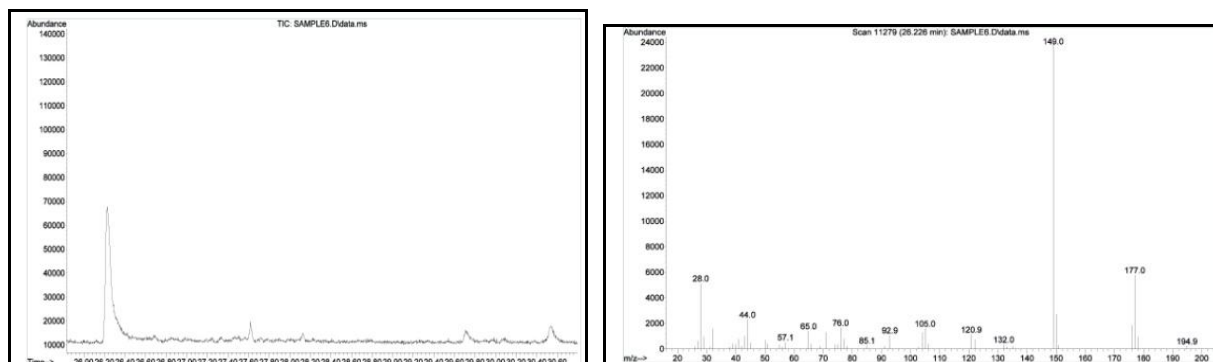


Fig. 14 GC-MS spectra of Rh-B using CNA composite sample.

Table 3 Various photoproducts of Rh-B formed in GC-MS analysis over CNA sample.

S.No	Degraded product name	Retention time(min)	Molecular formula	Molecular weight
1	Hydrazine	1.49	H ₄ N ₂	32
2	Propane,1-methoxy-2-methyl-	3.09	C ₅ H ₁₂ O	88
3	1,4-Dioxan-2-ol	9.04	C ₄ H ₈ O ₃	104
4	Diethyl phthalate	26.22	C ₁₂ H ₁₄ O ₄	222
5	1,2-Benzene dcarboxylic acid,2-ethoxy-2-oxethyl ethyl ester	27.61	C ₁₄ H ₆ O ₆	280
6	Phthalic acid, monoamide, N-ethyl-N-(3-methylphenyl)- ethyl ester	27.62	C ₁₉ H ₂₁ NO ₃	311

In GC-MS chromatogram of CNA mediated system consists of six primary peaks at retention times less than 27.62 minutes. One of the peaks corresponds to the initial Rh-B. The other peaks are those of the intermediate photoproducts formed. Table 3 presents the retention time and the photoproducts obtained by MS spectra over CNA composite photocatalysts.

IV. CONCLUSIONS

The present work has shown the effectiveness of visible light induced CNA and CNPANI composites for the photodegradation of Rh-B dye in aqueous solution. From UV-Visible absorption data CNA composite could be achieved 82 % degradation of Rh-B within 120 min irradiation in the presence of sunlight. The kinetics data agreed well with pseudo-first order kinetics in both the cases. The degradation rate constant of CNA composite can be estimated to be 2.13 times higher than that of polymer doped composite CNPANI. The complete mineralization of dye can be confirmed by GC-MS analysis. Thus it can be conclude that CNA can be used as highly efficient metal-free photocatalyst for the removal of Rh-B than polymer doped g-C₃N₄ composite photocatalyst.

REFERENCES

- [1] M.K Purkait, V.D Kumarb and D Maity, (2009), Treatment of leather plant using NF followed by RO and permeate flux prediction using artificial neural work, *Chemical Engineering Journal*, **151**: 275-285.
- [2] A.N Rao, B Sivasankar and V Sathasivam, (2009), Kinetic studies on the photocatalytic degradation of Direct Yellow 12 in the presence of ZnO catalyst, *Journal of Molecular Catalysis.A: Chemical*, **306**: 77-81.
- [3] M. Vautier, C. Guillard and J.M Hermann, (2001), Photocatalytic degradation of dyes in water: case study

- of Indigo and Indigo Carmine, *Journal of Catalysis*, **201**: 46-49.
- [4] T. Sauer, G.C. Neto, H.J Jose and R.F.P.M. Moreira, (2002), Kinetics of photocatalytic degradation of reactive dyes in TiO₂ slurry reactor, *Journal of Photochemistry and Photobiology.A*, **149**: 147-154.
- [5] Z.Tang and H. An, (1995), Photocatalytic oxidation of commercial dyes in aqueous solutions, *Chemosphere*, **31**: 4157-4170.
- [6] A.Y. Liu and R.M. Wentzovitch, (1994), Stability of carbon nitride solids, *Physical Review B*, **50**: 10362-10365,
- [7] B.H. Long, Z.X. Ding and X.C Wang, (2013), Carbon nitride for the selective oxidation of aromatic alcohols in water under visible light, *ChemSusChem*, **6**: 2024-2078.
- [8] J. Qin , S.Wang ,H. Ren ,Y. Hou and X.Wang , (2015), 'Photocatalytic reduction of CO₂ by graphitic carbon nitride polymers derived from urea and barbituric acid', *Applied catalysis B:Environmental*, **179**:1-8.
- [9] Q.J.Xiang ,J.G.Yu and M Jaroniec ,(2011), 'Preparation and enhanced visible-light photocatalytic H₂-production activity of graphene/C₃N₄ composites', *Journal of Physical Chemistry C*, **115** : 7355- 7363.
- [10] M.Zhang , J.Xu.R.Zong and Y. Zhu , (2014), 'Enhancement of visible light photocatalytic activities via porous structure of g-C₃N₄, *Applied Catalysis B:Environmental*, **147** : 229-235.
- [11] G. Liao, S. Chen ,X. Quam ,H. Yu and H. Zhao , (2012), 'Graphene oxide modified g-C₃N₄ hybrid with enhanced photocatalytic apability under visible lightirradiation', *Journal of Materials Chemistry*, **22**: 2721-2726.
- [12] W. Zheng ,M. Angelopoulos ,A.J. Epstein , and A.G. MacDiarmid (1997), ' Experimentalevidence for hydrogen bonding in polyaniline: Mechanism of aggregate formation and dependency on oxidation state', *Macromoleules*, **30**: 2953.